Dynamical properties of Au from tight-binding molecular-dynamics simulations

F. Kirchhoff,[1] M. J. Mehl,[2] N. I. Papanicolaou,[3] D. A. Papaconstantopoulos,[2] and F. S. Khan[1]
[1]*Department of Electrical Engineering, Ohio State University, Columbus, Ohio 43210*
[2]*Center for Computational Materials Science, Naval Research Laboratory, Washington DC 20375-5000*
[3]*Department of Physics, Solid State Division, University of Ioannina, P.O. Box 1186, GR-45110 Ioannina, Greece*
(Received 22 December 1999; revised manuscript received 11 January 2001; published 9 April 2001)

We studied the dynamical properties of Au using our previously developed tight-binding method. Phonon-dispersion and density-of-states curves at $T=0$ K were determined by computing the dynamical matrix using a supercell approach. In addition, we performed molecular-dynamics simulations at various temperatures to obtain the temperature dependence of the lattice constant and of the atomic mean-square displacement, as well as the phonon density-of-states and phonon-dispersion curves at finite temperature. We further tested the transferability of the model to different atomic environments by simulating liquid gold. Whenever possible, we compared these results to experimental values.

DOI: 10.1103/PhysRevB.63.195101 PACS number(s): 71.15.Ap, 71.15.Pd, 63.20.−e, 65.40.De

I. INTRODUCTION

Over the last two decades, atomistic simulations have become an increasingly important tool for modeling in many areas of condensed-matter physics and material science. The most challenging problem in computer-based nano-scale simulations of real materials is to find an accurate and transferable model for the atomic interactions that reproduces the energetic and electronic properties of the material. A whole hierarchy of models for atomic interactions have been developed, ranging from simple empirical potentials to sophisticated first-principles calculations based on density functional theory (DFT). Although DFT methods are very accurate and have been successfully applied to the study of a broad range of materials and systems, they are computationally very demanding. Even with today's state-of-the-art computers, DFT simulations with more than 100 atoms are challenging. Empirical potentials, on the other hand, are less demanding and have been used to simulate systems with millions of atoms. This advantage is, however, to be weighed against a loss in accuracy and transferability.

Several empirical potential methods have been used in the past to simulate metallic systems: the embedded-atom method, the effective-medium theory, Finnis-Sinclair potentials, and the second-moment approximation to the tight-binding model.[1] The decade has seen the emergence of a method that lies between first principles and empirical potentials: the so-called tight-binding (TB) molecular-dynamics method. It is more accurate than the empirical potential methods because it explicitly describes the electronic structure of the system. TB is roughly three orders of magnitude faster than DFT-based methods due to the much smaller size of the secular equation, which makes the N^3 issue more tolerable. The TB method has been used to study a broad range of materials.[2]

Recently, the NRL group proposed an alternative formulation of the TB method, which was shown to work well for transition metals,[3] simple metals,[4] and semiconductors.[5] This approach has been successful in determining static properties such as structural energy differences, elastic constants, vacancy formation energies, and surface energies.

Although static calculations are very useful for determining many fundamental properties of materials, such calculations are limited to properties at $T=0$ K. Most problems in real materials involve processes that occur at finite temperatures. The purpose of the present work is to demonstrate that our TB model can successfully be applied to the study of the dynamical and finite temperature properties of a representative material, gold. Our previous TB parametrization of gold[3] was highly successful in predicting structural properties. We have improved upon this parametrization in this paper. This provides us with an ideal test case for demonstrating the power of the method.

We tested our TB parameters by calculating the elastic properties and comparing to first-principles calculations and experiment. We also found the phonon-dispersion curves and density of states (DOS) at $T=0$ K by calculating the dynamical matrix using a supercell method.[6] In addition, we performed molecular-dynamics (MD) simulations at various temperatures to obtain the temperature dependence of the lattice constant and of the atomic mean-square displacement, as well as the electronic and phonon DOS and the phonon-dispersion curves at finite temperatures and a simulation of the liquid phase. Whenever possible, we compare these results to experimental data.

II. TECHNICAL DETAILS

A. Fitting procedure for Au

Details about our TB model can be found in Ref. 3. In this paper we used a new TB parametrization for Au,[7] which works well even at very small interatomic distances. The parameters of the model are fitted to reproduce data from DFT calculations: band structures and total energy as a function of volume for fcc, bcc, and simple cubic (sc) structures. In the present case the database included ten (10) fcc structures, six (6) bcc structures, and five (5) sc structures. The calculations were performed using the general potential linearized augmented plane-wave (LAPW) method,[8,9] using the Perdew-Wang[10] parametrization of the local density approximation.[11] In addition, care was taken to include energies at very small volumes (down to 60% of the equilibrium

volume) in the fitting database. This turned out to be very important in order to have parameters that could be used in the wide range of interatomic distances that occur during MD simulations. Finally, it should be stressed that no experimental data is used to determine the parameters of the model.

B. DoD-TBMD code

Except as noted, the results presented in this paper were obtained using the DoD-parallel tight-binding molecular-dynamics (TBMD) code developed as part of the computational chemistry and materials science (CCM) contribution to the Common HPC Software Support Initiative (CHSSI). This program was written with the goal of performing molecular-dynamics simulations of metallic systems. Although initially written to run with our TB Hamiltonian,[3] this code is in fact model independent.[12] The electronic structure is calculated using either an $O(N^3)$ method such as diagonalization, or by using an $O(N^2)$ method called the kernel polynomial method (KPM).[13,14] The code has been written for both scalar and parallel computers. The parallel parts of the code have been written using a message-passing programming model relying on the MPI library to deal with communications.[15]

C. Simulation details

To compute the dynamical matrix we used an fcc supercell of 1331 atoms, obtained by replicating a primitive fcc cell 11 times along the three primitive lattice vectors. Periodic boundary conditions are applied throughout this work. In the MD simulations, the system consists of an fcc supercell of 343 atoms, obtained by replicating a primitive fcc cell seven times along the three primitive lattice vectors. The Brillouin zone (BZ) is sampled using the Γ point. We checked that this is a reasonable approximation even for a metal: the lattice constant, bulk modulus, and elastic constants obtained from the 343 atom supercell and Γ-point sampling are within 10% of the values obtained using a primitive cell and a well-converged *k*-point set. The MD simulations were started with atoms arranged on an fcc lattice and random velocities drawn from a Boltzmann distribution for a temperature 2 T. The MD simulation was performed in the microcanonical ensemble, so at equilibrium the temperature of the lattice averaged to *T*, and the ''potential energy'' of the system was raised by an amount $3/2\ Nk_BT$, where *N* is the number of atoms and k_B is Boltzmann's constant. The equations of motion were integrated using the Verlet algorithm and a time step of $\Delta t = 2$ fs, giving a total-energy conservation within $\Delta E/E = 10^{-5}$. The system was equilibrated at the desired temperature for 1500 time steps (3 ps). Typically, another 1500 additional steps were performed to calculate time averages. The finite size of the simulation cell and the finite number of time steps in the simulation implies that the instantaneous temperature of the cell, computed from the kinetic energy, fluctuated around some average temperature, which was not necessarily the target temperature. For the simulations conducted at a target temperature of 300 K, we found that the average temperature after the system reached equilibrium was 301 K, with a standard deviation of 8 K. At 600 K, we found the average temperature to be 604 K, with standard deviation 20 K, and at 1200 K, we found 1212 and 113 K, respectively.

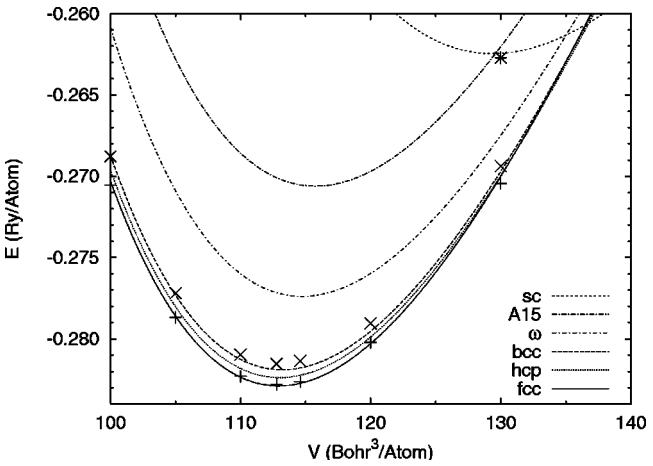

FIG. 1. Equation of state for selected crystal structures of gold using the tight-binding parameters discussed in the text. All coordinates are relaxed at each volume. The points are the first-principles LAPW energies used in the fit. From bottom to top, the ordering of the structures is fcc (LAPW symbol +), hcp, bcc (LAPW symbol ×), hexagonal ω, A15, and simple cubic (sc, LAPW symbol *).

For the computation of the temperature dependence of the lattice constant, we used a 64 atom fcc supercell and sampled the BZ with four *k* points. For each volume and temperature we ran a Langevin dynamics simulation[16] for 2.5 ps, using a time step of 5 fs and a friction parameter $\gamma = 0.05\ \mathrm{fs}^{-1}$.

III. RESULTS AND DISCUSSION

A. Equation of state

In Fig. 1 we present the energy versus volume curves for a selection of crystal structures, calculated using the static TB code.[17] The LAPW total energies for the fcc, bcc, and sc structures, which were used in the fit, are also plotted on the graphs. We find that the TB Hamiltonian predicts that the equilibrium fcc structure has a lower energy than any other structure yet tested, consistent with experiment and first-principles calculations, and confirming the robustness of the Hamiltonian.

B. Elastic properties

The elastic properties of bulk fcc Au were calculated using our TB parameters by means of the standard finite-strain method[18,19] and the static code. The results are shown in Table I, along with comparisons to experimental data[20] and the results of first-principles LAPW calculations. The latter calculations were also performed using the Perdew-Wang local-density approximation (LDA) parametrization.[10] The TB calculations reproduce the LAPW results very well and are in good agreement with the experimental data.

C. Phonons at $T = 0$ K

We determined the phonon dispersion curves and density of states (DOS) of fcc Au by computing the dynamical ma-

TABLE I. Bulk modulus and elastic constants (in GPa) for Au computed using our TB model compared to the results of LAPW calculations and experimental data. All calculations are performed at the experimental room-temperature volume, the measured elastic constants are taken from the compilation of Simmons and Wang (Ref. 20).

	B	C_{11}-C_{12}	C_{11}	C_{12}	C_{44}
TB	181	21	195	174	40
LAPW	182	27	200	173	33
Exp.	169	30	189	159	42

trix. This was achieved by using a large supercell, in our case containing 1331 atoms, and calculating the forces on all atoms in response to the displacement of the atom at the origin. Provided this displacement is small enough it is possible to construct the real-space dynamical matrix using finite differences and compute the dynamical matrix by a Fourier series.[6]

The high-symmetry direction phonon-dispersion curves for Au at $T=0$ K are shown in Fig. 2(a), together with experimental data.[21] The overall structure of the dispersion curves is well reproduced. The low-frequency transverse modes are in excellent agreement with experiment. The longitudinal higher-frequency modes, however, are systematically too high close to the BZ edge.

The phonon DOS is presented in Fig. 2(b), together with experimental results. The DOS has two main peaks. From 0 to 3.5 THz, the theoretical DOS reproduces the experimental data very well. In contrast, in the region 4–5 THz, the position of the high-frequency peak in the theoretical curve is overestimated by about 0.5 THz compared to experiment, consistent with the discrepancy in the frequency of the high-frequency longitudinal modes noted above.

We checked that the observed discrepancies are not an artifact of the supercell method used to calculate the dynamical matrix. In particular, we made sure that an $11\times11\times11$ supercell is large enough to converge the dynamical matrix. A first check is given by the slopes of the dispersion curves as $k\rightarrow0$, which are related to the elastic constants. We found that the slopes were consistent with our computed elastic

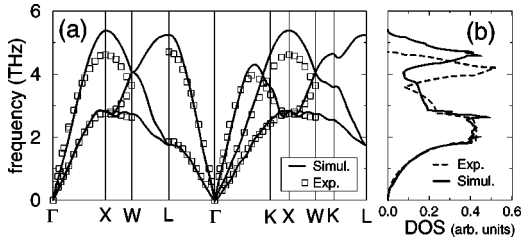

FIG. 2. (a) Phonon-dispersion curves for Au at $T=0$ K, plotted along high-symmetry directions in the BZ. Lines are spline fits to the theoretical TB data, open squares are experimental data points. (Ref. 21) (b) Phonon density-of-states (DOS) for Au at $T=0$ K. The full line is the theory result using our TB model, while the dotted line is a fit to the experimental values. (Ref. 21) The dispersion curves and DOS were calculated from the dynamical-matrix computed using an fcc supercell containing 1331 atoms.

TABLE II. Selected phonon frequencies (in THz) at high-symmetry points in the Brillouin zone. The calculated TB and LAPW frequencies were obtained with the frozen phonon method in cells with two or four atoms.

	X(L)	X(T)	L(L)	L(T)	W(L)	W(T)
TB	5.29	2.87	5.35	1.91	2.66	4.01
LAPW	4.43		4.53			
Exp. (Ref. 21)	4.60	2.72	4.69	1.85	2.63	3.62

constants (see Table I). Another check is to compute the frequency of BZ-edge phonons using the frozen-phonon method[22] for a two or four atom unit cell, using the static code to calculate the total energies. The computed BZ-edge phonon frequencies are shown in Table II. They are in perfect agreement with the frequencies derived from the dispersion curves obtained using the dynamical-matrix method (see Fig. 2), hence, confirming the accuracy of the latter approach. Finally, using the first-principles LAPW method, we calculated the phonon frequencies at X and L and found very good agreement with experiment as shown in Table II. We therefore conclude that the overestimate of our calculated longitudinal phonon frequencies near the BZ edge is a shortcoming of our TB parameters. An obvious approach to overcome this problem and improve the agreement with experiment would be to include the LAPW frequencies at X and L in our fitting database. Nevertheless, we note that our TB results for the dispersion curves present a substantial improvement over results obtained using the second-moment approximation to TB.[1]

D. Electronic density of states at finite temperature

The TBMD code computes all of the eigenvalues of the system at each time step, making it simple to determine electronic properties such as the density of states as a function of temperature. In Fig. 3 we show the electronic DOS at several

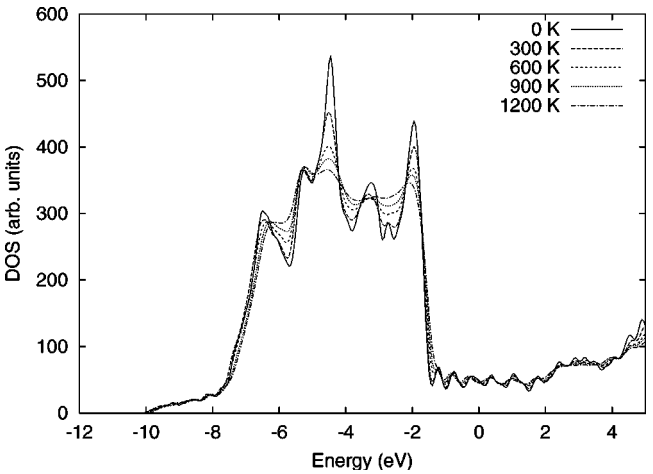

FIG. 3. Temperature dependence of the electronic density of states of gold, calculated using the eigenvalues generated by the TBMD code, and averaged over ten time steps, as outlined in the text.

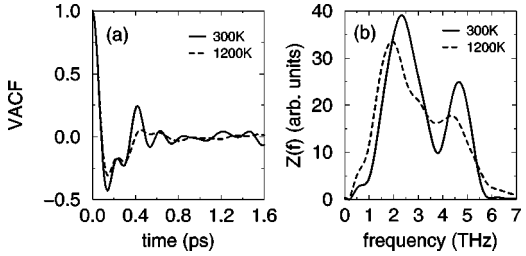

FIG. 4. (a) Velocity-velocity auto-correlation functions (VACF) of Au calculated from molecular-dynamics simulations at 300 and 1200 K using our TB model. (b) Finite-temperature phonon spectral-density (PSD) $Z(f)$ for Au at 300 and 1200 K. The PSD was computed by Fourier-transform of the VACF shown in (a).

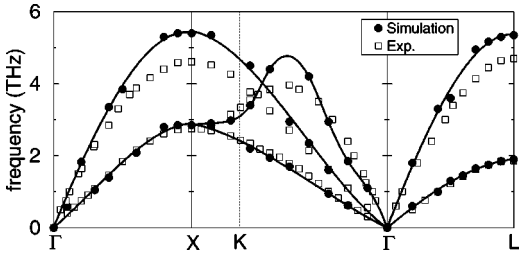

FIG. 5. Finite-temperature phonon-dispersion curves along the high-symmetry directions in the BZ, for Au at 300 K calculated using molecular-dynamics simulations based on our TB model. Filled circles are theoretical data, lines are polynomial fits to theoretical data, open squares are experimental data points. (Ref. 21) The dispersion curves were computed by Fourier transform of the time-dependent wave-dependent VACF (see text).

temperatures. For each temperature, we saved the eigenvalues for ten different time steps. The DOS was then calculated assuming a Fermi distribution, and the resulting DOS were averaged. We see that the dominant effect of increasing temperature is to reduce the peaks in the electronic DOS spectrum.

E. Phonons at finite temperature

We determined the phonon-dispersion curves and spectral density of fcc Au at finite temperatures by performing MD simulations. In Fig. 4(a) we show the velocity-velocity auto-correlation functions (VACF) obtained from the MD simulation at 300 and 1200 K. We see that increasing temperature damps out the oscillations in the VACF.

The finite-temperature phonon spectral density (PSD) can be obtained from the Fourier transform of the VACF,[23] as shown in Fig. 4(b). The PSD has the two well-defined peaks, consistent with the DOS at $T=0$ K. The position of the peaks is also in agreement with the theoretical data at $T=0$ K. The limited resolution in the finite-temperature PSD, due to the short length of the MD simulation, makes a detailed comparison with experiment difficult. It should also be pointed out that the PSD is proportional to the phonon DOS only in a harmonic solid; one should therefore be cautious when comparing the PSD to the phonon DOS, in particular at high temperature. We believe this may explain the difference in height between the two peaks in the PSD, in contrast to the $T=0$ K phonon DOS, where both peaks have about the same height. Comparison of the PSD at 300 and 1200 K clearly reveals the effect of temperature: a clear shift of phonon frequencies to lower values and a broadening of the peaks in the PSD.

To compute the phonon-dispersion curves we calculate the PSD from the Fourier transform of the velocity- and position-dependent auto-correlation function. Details of this computational procedure can be found elsewhere.[24] The dispersion curves along high-symmetry directions in the BZ at 300 K are reproduced in Fig. 5. The comparison with experimental data reveals the same discrepancies as in the $T=0$ K dispersion curves: the high-frequency longitudinal modes are overestimated close to the BZ edge.

We determined the temperature dependence of phonon frequencies by performing MD simulations at 300, 600, 900, and 1200 K where for each temperature we fix the volume at the experimental value. In Table III we show the frequency of selected BZ-edge phonons as a function of temperature. These frequencies were calculated as described above for the 300 K case.

As expected, the frequency of phonons decreases with temperature. For the modes we computed the change was of the order of 0.2–0.3 THz, the transverse mode at L exhibiting the largest decrease. Part of this variation is probably due to an increase in volume as the temperature increases. It should be noted that using MD to compute the phonon dispersion curves at finite temperature can be particularly useful in systems where a particular crystal structure is unstable at $T=0$ K (bcc Ti is one example) and where the dynamical-matrix method will predict unstable phonon modes. MD simulation may also be useful to determine the vibrational properties of systems for which an experimental study may be difficult, e.g., clusters or nanocrystals.

F. Thermal expansion

To determine the theoretical thermal expansion coefficient α we use the following definition for α:

$$\alpha = \frac{1}{3B}\left(\frac{\partial P}{\partial T}\right)_V . \tag{1}$$

This definition requires the calculation of the pressure as a function of temperature for a fixed volume. We perform MD simulations at 300, 600, 900, and 1200 K, keeping the volume fixed at the experimental value at room temperature (lattice constant $a=4.08$ Å). For each temperature we selected ten independent configurations from the trajectories

TABLE III. Selected phonon frequencies (in THz) at high symmetry points in the Brillouin zone, calculated as a function of temperature (T in Kelvin) from MD simulations using our TB model.

T (K)	X(T)	X(L)	L(T)	L(L)
300	2.85	5.40	1.90	5.35
600	2.82	5.35	1.80	5.22
900	2.77	5.28	1.70	5.18
1200	2.65	5.20	1.60	5.15

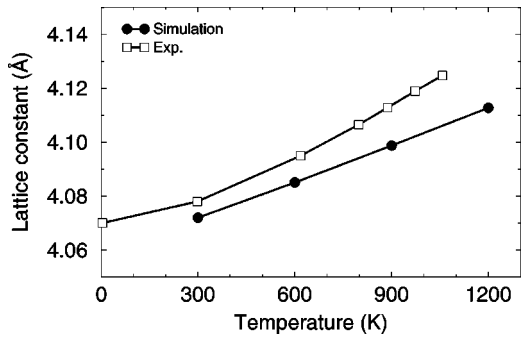

FIG. 6. Lattice constant of Au as a function of temperature. The black circles are the results of the molecular-dynamics simulations using our TB model, open squares are the experimental data (Ref. 26).

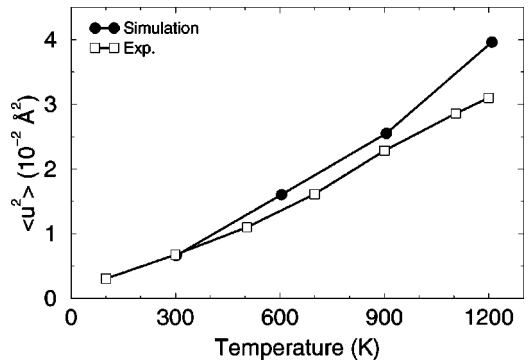

FIG. 7. Mean-square displacement of Au as a function of temperature. The filled circles are the results of the molecular-dynamics simulations using our TB model, empty squares are the experimental points (Ref. 27).

generated by the MD and computed the instantaneous pressure. We found that ten configurations per temperature were enough to get the average pressure with an error margin of $\sim 5\%$. If, in Eq. (1), we assume the pressure varies linearly as a function of temperature, and if for B we use the theoretical value of the bulk modulus at $T=0$ K and at the experimental volume, we get $\alpha = 11\times 10^{-6}\mathrm{K}^{-1}$. This underestimates the experimental value of $14\times 10^{-6}\mathrm{K}^{-1}$ at 300 K.[25]

An alternative definition of α is given by:

$$\alpha = \frac{1}{3V}\left(\frac{\partial V}{\partial T}\right)_P . \tag{2}$$

To check the calculation of α based on Eq. (1) we computed α using this latter definition. This requires MD simulations for several volumes (typically three or four) for a given temperature. For each volume V we compute the average pressure P. The equilibrium volume at each temperature is found by interpolating $P(V)$ to find the volume that gives zero pressure. We performed this procedure at 300, 600, 900, and 1200 K to find $V(T)$.

In Fig. 6 we show the lattice constant as a function of temperature as derived from the simulations, compared to experimental results.[26] The overall agreement with experiment is good, given that the theoretical data is well within 1% of experiment in the temperature range we simulated.

From Fig. 6 we can see that it is reasonable to assume that the volume varies linearly as a function of T. So by using Eq. (2), we get $\alpha = 11\times 10^{-6}\mathrm{K}^{-1}$, in agreement with our previous estimate based on Eq. (1).

G. Mean-square displacement

We used the atomic positions generated by the MD simulations performed for several temperatures at the corresponding experimental lattice constants to compute the atomic mean-square displacement (MSD). In Fig. 7 we compare the temperature dependence of our computed MSD with experimental data.[27] The agreement with experiment is excellent up to 900 K, at higher temperatures the theoretical MSD gets larger than the experimental values. Again, it should be noted that the results of our calculation are in much better agreement with experiment compared to previous work using the second-moment approximation to TB.[1]

H. Liquid Au

To further test the transferability of our model to different atomic environments we studied the liquid phase of Au. The simulation was performed with 200 atoms in a periodic fcc unit cell. The density of the sample was chosen to be equal to the experimental value of 16.746 g cm^{-3} at 1773 K.[28] One thousand (1,000) MD steps were used to equilibrate the system. Statistical averages of structural properties were computed from data collected from the next two thousand (2,000) MD steps. The radial distribution function $g(r)$ obtained from our simulation (shown in Fig. 8) is found to be in very good agreement with experimental data.[29]

We also calculated the electronic DOS of liquid gold at 1773 K, using the same procedure as in the solid. The result is shown in Fig. 9. While the overall shape of the DOS, including the width, is similar to Fig. 3, the high temperature and loss of symmetry has destroyed most of the peak structure. However, two new peaks appear at low energies, probably due to the lack of periodicity in the liquid.

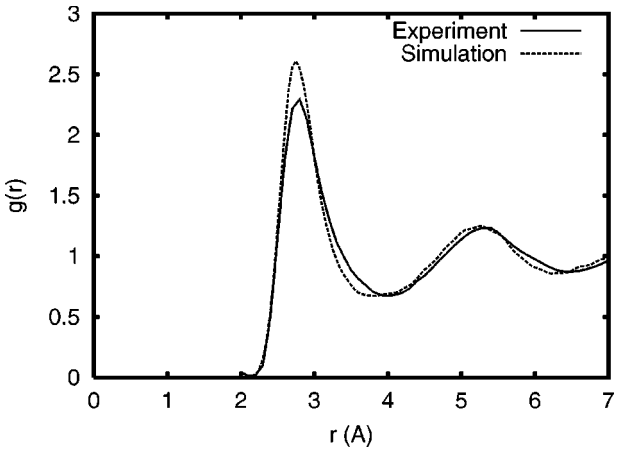

FIG. 8. Pair-correlation function $g(r)$ of liquid gold at 1773 K. The dotted line is the result of molecular-dynamics simulations using our TB model, the full line is the experimental result (Ref. 29).

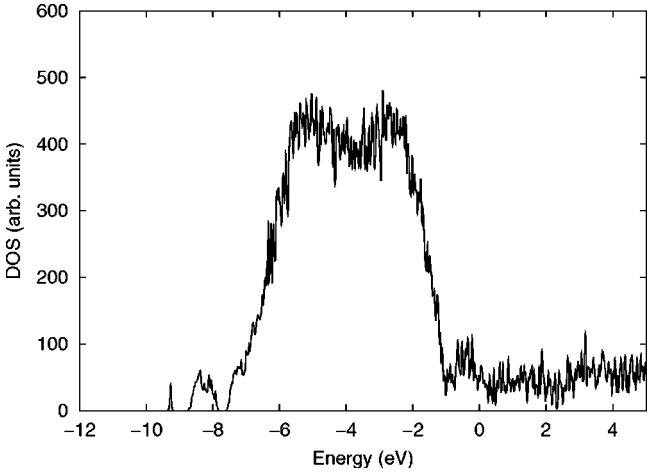

FIG. 9. Electronic density of states of liquid gold at $T=1773$ K, using the same method as in Fig. 3.

IV. CONCLUSION

We presented results of simulations of bulk fcc Au using our tight-binding model. Our TB Hamiltonian was used to compute the elastic constants of bulk Au, which were in very good agreement with the results of LDA calculations and experimental data. Using a supercell method to compute the dynamical matrix, we determined the phonon-dispersion curves and phonon density of states of Au at $T=0$ K. Our calculated dispersion curves are in good agreement with experimental data, except for a tendency to overestimate the frequency of longitudinal modes close to the Brillouin-zone edge. We checked that this discrepancy is not a consequence of the method used to calculate the phonon frequencies. In addition, we performed molecular-dynamics simulations at various temperatures to compute the phonon density-of-states and phonon-dispersion curves at finite temperature. The molecular-dynamics simulation were also used to obtain the temperature dependence of the lattice constant and of the atomic mean-square displacement. Both quantities were found to be in good agreement with experimental data. Finally, we performed an MD simulation of the liquid phase of Au and obtained a radial distribution function in very good agreement with experiment. We believe these results demonstrate that our TB model, using parameters generated by the same procedure,[30] can successfully be applied to the study of dynamical- and finite-temperature properties of other metals.

ACKNOWLEDGMENTS

M. J. M. and D. A. P. were supported by the U. S. Office of Naval Research. N. I. P. acknowledges partial support from NATO Grant No. CRG-940118. The development of the STATIC and DOD-TBMD codes was supported in part by the U. S. Department of Defense Common HPC Software Support Initiative (CHSSI). This work was supported in part by a grant of HPC time from the DoD HPC Center, for computations on the IBM SP2 and SGI Origin at the Aeronautical Systems Center, Wright-Patterson Air Force Base, Dayton, OH. F.K. was supported in part by U.S. Department of Energy-Basic Energy Sciences, Division of Materials Sciences.

[1] G. C. Kallinteris, N. I. Papanicolaou, G. A. Evangelakis, and D. A. Papaconstantopoulos, Phys. Rev. B **55**, 2150 (1997), and references therein.

[2] C. M. Goringe, D. R. Bowler, and E. Hernandez, Rep. Prog. Phys. **60**, 1447 (1997); M. J. Mehl and D. A. Papaconstantopoulos, in *Computational Materials Science*, edited by C. Fong (World Scientific, Singapore, 1998).

[3] D. A. Papaconstantopoulos and M. J. Mehl, Phys. Rev. B **54**, 4519 (1996).

[4] S. H. Yang, M. J. Mehl, and D. A. Papaconstantopoulos, Phys. Rev. B **57**, R2013 (1998).

[5] D. A. Papaconstantopoulos, M. J. Mehl, S. C. Erwin, and M. R. Pederson, *Tight-binding Approach to Computational Material Science*, edited by P. E. A. Turchi, A. Gonis, and L. Colombo, MRS Symposia Proceedings No. 491 (Materials Research Society, Pittsburgh, 1998), p. 221.

[6] See for example, G. J. Ackland, M. C. Warren, and S. J. Clark, J. Phys.: Condens. Matter **9**, 7861 (1997) and references therein.

[7] The gold parameters used in this paper are available from the authors, or at http://cst-www.nrl.navy.mil/bind/au_par_99

[8] O. K. Andersen, Phys. Rev. B **12**, 3060 (1975).

[9] D. Singh, H. Krakauer, and C. S. Wang, Phys. Rev. B **34**, 8391 (1986).

[10] J. P. Perdew and Y. Wang, Phys. Rev. B **45**, 13 244 (1992).

[11] W. Kohn and L. J. Sham, Phys. Rev. A **140**, 1133 (1965).

[12] We have tested the code with a variety of TB models found in the literature. Adding a new model requires only minor changes to the code.

[13] R. N. Silver, H. Roeder, A. F. Voter, and J. D. Kress, J. Comput. Phys. **124**, 115 (1996); A. F. Voter, J. D. Kress, and R. N. Silver, Phys. Rev. B **53**, 12 733 (1996).

[14] In the present work the size of the simulated systems is small enough that $O(N^3)$ methods are faster than $O(N^2)$ KPM methods.

[15] More details about the DoD-parallel tight-binding molecular-dynamics code can be found at the following URL: http://cst-www.nrl.navy.mil/bind/dodtb/

[16] N. Binggeli and J. R. Chelikowsky, Phys. Rev. B **50**, 11 764 (1994).

[17] For more information about the static TB code, see http://cst-www.nrl.navy.mil/bind/static/

[18] M. J. Mehl, J. E. Osburn, D. A. Papaconstantopoulos, and B. M. Klein, Phys. Rev. B **41**, 10 311 (1990); **42**, 5362E (1991).

[19] M. J. Mehl, B. M. Klein, and D. A. Papaconstantopoulos, in, *Intermetallic Compounds: Principles and Applications*, edited by J. H. Westbrook and R. L. Fleischer (Wiley, London, 1995), Vol. 1, Chap. 9.

[20] G. Simmons and H. Wang, *Single Crystal Elastic Constants and Calculated Aggregate Properties: A Handbook*, 2nd ed. (MIT Press, Cambridge, MA, 1971).

[21] J. W. Lynn, H. G. Smith, and R. M. Nicklow, Phys. Rev. B **8**, 3493 (1973).
[22] K.-M. Ho, C. L. Fu, B. N. Harmon, W. Weber, and D. R. Hamann, Phys. Rev. Lett. **49**, 673 (1982).
[23] The Fourier transform of the VACF gives the spectral density that is proportional to the phonon density of states in an harmonic solid.
[24] N. I. Papanicolaou, I. E. Lagaris, and G. A. Evangelakis, Surf. Sci. **337**, L819 (1995).
[25] Y. S. Touloukian, in *A Physicist's Desk Reference: The Second Edition of the Physics Vade Mecum*, edited H. L. Anderson (American Institute of Physics, New York, 1989), p. 345.
[26] W. B. Pearson, *A Handbook of Lattice Spacings and Structures of Metals and Alloys* (Pergamon, New York, 1958).
[27] E. A. Owen and R. W. Williams, Proc. R. Soc. London, Ser. A **188**, 509 (1947).
[28] D. J. Steinberg, Metall. Trans. **5**, 1341 (1974).
[29] Y. Waseda, *Structure of Non-Crystalline Materials* (McGraw-Hill, New York, 1980).
[30] Parameters for other elements (Refs. 3–5) are available at http://cst-www.nrl.navy.mil/bind/